THE JOURNAL OF PHYSICAL CHEMISTRY LETTERS
A JOURNAL OF THE AMERICAN CHEMICAL SOCIETY

pubs.acs.org/JPCL

Letter

Scanning Nuclear Spin Level Anticrossings by Constant-Adiabaticity Magnetic Field Sweeping of Parahydrogen-Induced ^{13}C Polarization

Baptiste Joalland* and Eduard Y. Chekmenev*

Cite This: *J. Phys. Chem. Lett.* 2022, 13, 1925−1930

Read Online

ACCESS | Metrics & More | Article Recommendations | Supporting Information

ABSTRACT: The polarization transfer between ^{1}H protons and ^{13}C heteronuclei is of central importance in the development of parahydrogen-based hyperpolarization techniques dedicated to the production of ^{13}C-hyperpolarized molecular probes. Here we unveil the spin conversion efficiency in the polarization transfer between parahydrogen-derived protons and ^{13}C nuclei of an ethyl acetate biomolecule, formed by the homogeneous hydrogenation of vinyl acetate with parahydrogen, obtained by applying constant-adiabaticity sweep profiles at ultralow magnetic fields. The experiments employed natural C-13 abundance. Spin level anticrossings can be detected experimentally using a scanning approach and are selected to improve the polarization transfer efficiency. ^{13}C polarization of up to 12% is readily achieved on the carbonyl center. The results demonstrate the simplicity, reproducibility, and high conversion efficiency of the technique, opening the door for a refined manipulation of hyperpolarized spins in both basic science experiments (*e.g.*, state-selected spectroscopy in the strong-coupling regime) and biomedical nuclear magnetic resonance applications.

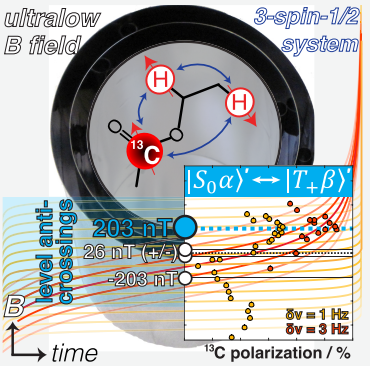

Nuclear magnetic resonance (NMR) hyperpolarization can transiently increase the nuclear spin polarization (P) well beyond the thermal equilibrium level.[1] The massive P gain is realized by the corresponding four- to six-order gain in NMR signals, enabling new applications of magnetic resonance.[2−6] The biomedical application of hyperpolarized (HP) biocompatible molecules is the main driver behind the development of NMR hyperpolarization techniques.[7,8] Highly polarized biologically compatible molecules can be employed for their visualization *in vivo*.[9,10] For example, HP [1-^{13}C]pyruvate can be utilized for the detection of its aberrant metabolism in cancer and other metabolically challenged diseases.[10,11] HP [1-^{13}C]-acetate has been employed for brain, liver, and other *in vivo* molecular imaging applications.[12−15]

Dissolution dynamic nuclear polarization (d-DNP)[3,16] is the leading hyperpolarization technique for the production of ^{13}C HP contrast agents for *in vivo* applications. However, it has a number of disadvantages including high cost (∼$2 M clinical-scale device), cryogenic operation, and slow HP contrast agent production speed (∼1 h). Hyperpolarization techniques relying on parahydrogen (p-H_2) addition to an unsaturated substrate[17] can potentially mitigate the limitations of d-DNP hyperpolarization technology.[4,18,19] As a result, the field of parahydrogen-induced polarization (PHIP) has been rapidly expanding.[20−25]

Reineri and coworkers have recently demonstrated PHIP side-arm hydrogenation (SAH), where p-H_2 is added to the ester side arm of [1-^{13}C]carboxylic acid.[26] Following p-H_2 pairwise addition, the polarization is transferred from the nascent p-H_2-derived protons to the [1-^{13}C]carbonyl nucleus.[26] Next, the ester moiety is cleaved, and the HP biomolecule is released in the aqueous medium.[26] The catalyst is left behind in the organic solvent layer;[26] alternatively, heterogeneous PHIP-SAH allows the catalyst-free preparation of HP biomolecules.[27−29] PHIP-SAH was successfully employed for the ^{13}C hyperpolarization of key metabolic probes: [1-^{13}C]pyruvate,[30,31] [1-^{13}C]acetate,[26,32] and [1-^{13}C]lactate.[33] PHIP-SAH represents a major advance in the field of PHIP because it enables a wide range of biomolecular carboxyl ^{13}C to retain the HP state for minutes, that is, the time frame suitable for *in vivo* applications.[18] Hence, PHIP-SAH-hyperpolarized [1-^{13}C]pyruvate has been successfully employed for coronary imaging[34] and sensing metabolic fluxes in cancer cells.[35]

The polarization transfer from the nascent p-H_2-derived protons to the ^{13}C nucleus is accomplished via adiabatic passage through nuclear spin level anticrossings (LACs). Magnetic field sweeping/cycling (MFS/C) is performed immediately after pairwise p-H_2 addition. The efficiency of polarization transfer depends on the size of the spin−spin couplings between the two p-H_2-derived protons and the ^{13}C nucleus, the ^{1}H and ^{13}C T_1 relaxation in ultralow magnetic fields, and the shape of the applied magnetic field passage profile. Historically, exponentially increasing MFC-programmed forms were demonstrated first for the production of hyperpolarized 2-hydroxyethyl propionate

Received: January 5, 2022
Accepted: February 11, 2022

https://doi.org/10.1021/acs.jpclett.2c00029
J. Phys. Chem. Lett. 2022, 13, 1925−1930

(HEP).[4,36] Manual MFC has been also demonstrated, where the HP sample is slowly pulled out from the submicrotesla magnetic field (typically created by μ-metal shield) into the Earth's magnetic field (*ca.* 50 μT).[37,38] Linear MFS has also been demonstrated.[39,40] Most recently, WEREWOLF (Whopping Enhancement Realized by Excitation With Oscillating Low Field) for the PHIP of heteronuclei has been introduced.[41] Each approach has its own merits. For example, manual MFC is simple to implement, albeit at the expense of polarization transfer efficiency and poor reproducibility. The other approaches are more instrumentation demanding because they require a programmable sequence, a magnet coil, and a coil driver to increment the static magnetic field in small steps or to apply oscillating waveforms.

Recently, constant-adiabaticity radio-frequency (RF) pulses for generating long-lived singlet spin states were introduced by Ivanov and coworkers.[42] This approach is not restricted to the design of optimal RF ramps for singlet-state experiments. It can also be used for the purpose of transferring HP spin order from directly polarized spins to targeted spins, as emphasized by these authors. In theory, up to 97% ^{13}C polarization can be reached. In practice, $P_{^{13}C} \approx 50\%$ and $P_{^{13}C} \approx 40\%$ have been demonstrated for HP [1-^{13}C]fumarate using MFC and MFS approaches, respectively, using a 1 s long sweep duration.[42]

In the spin systems with very long ^{1}H and ^{13}C T_1, for example, most notably HP [1-^{13}C]fumarate, the relaxation losses occurring during several seconds long MFC/S are inconsequential because the duration of the MFC/S procedure is substantially shorter than T_1. The HP state therefore remains well preserved during the polarization transfer step.[40,43] However, the long nascent proton T_1 of HP [1-^{13}C]fumarate is associated with the presence of a C=C bond, which is a somewhat rare example of a PHIP-produced HP biomolecule obtained via the hydrogenation of an unsaturated precursor with a C≡C bond. On the contrary, the PHIP-SAH approach enables the hyperpolarization of a much wider repertoire of molecular probes, including [1-^{13}C]pyruvate and [1-^{13}C]-acetate.[26] Unlike HP [1-^{13}C]fumarate, these HP contrast agents have substantially shorter T_1 constants in submicrotesla magnetic fields. As a result, fast and efficient MFC/S profiles are necessary to minimize T_1-related losses during the polarization transfer. Here we report on a series of experiments with constant-adiabaticity MFS to investigate the polarization transfer efficiency in HP ethyl acetate produced via pairwise p-H_2 addition to vinyl acetate (Scheme 1), thereby introducing PHIP-SAH moieties with a shorter T_1 of p-H_2 derived protons but a wider scope of biologically relevant molecular probes to a series of well-controlled adiabatic ultralow magnetic field manipulations performed in a systematic manner. Furthermore, this novel approach enables (1) the demonstration of magnetic field scanning to experimentally identify LACs with minimal knowledge of the coupling parameters hand in hand with (2) the demonstration of the utility of natural-abundance PHIP precursors (at 1.1% ^{13}C occurrence) with high levels of polarization allowing the sufficiently sensitive detection of ^{13}C hyperpolarization using a benchtop NMR spectrometer. Hence the entire development process of HP biomolecular contrast agents can be accomplished in any chemistry lab without the need for high-field NMR instrumentation or the purchase/synthesis of ^{13}C-labeled compounds.

Scheme 1. Parahydrogen (p-H_2) Pairwise Addition to Vinyl Acetate (VA), Leading to Ethyl Acetate (EA) with Two Nascent p-H_2-Derived Protons[a]

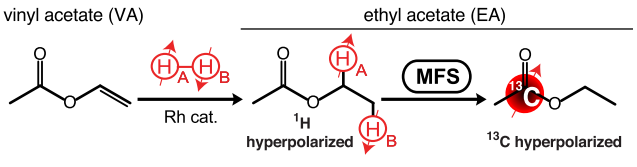

[a] ^{1}H polarization is transferred to ^{13}C nuclei present at natural abundance (1.1%) by magnetic field sweeping (MFS), with the carbonyl C1 as the main target for future imaging applications.

A schematic of the experimental setup is shown in Figure 1, including a typical time sequence for hydrogenation, low-field

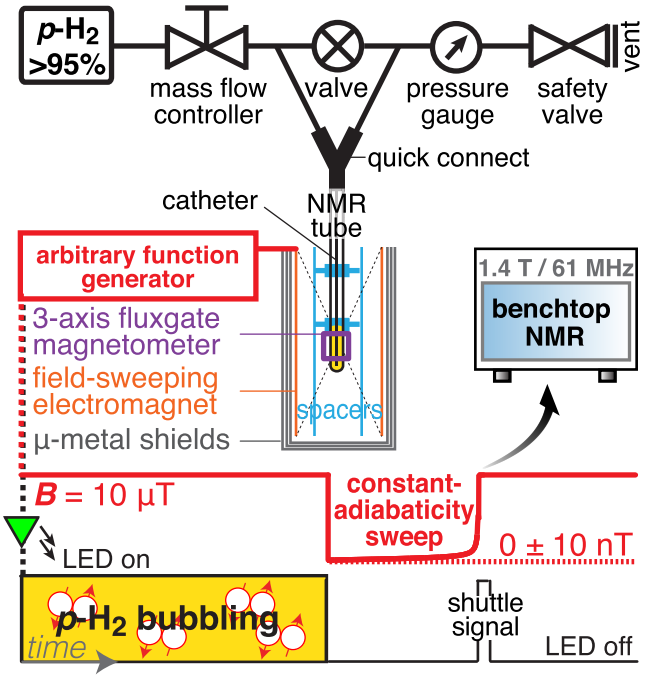

Figure 1. Schematic of the experimental setup to perform PHIP-SAH and measure ^{13}C polarization. (See the text for details.)

sweeping, and detection. The solution, containing 200 mM of vinyl acetate and 4 mM of catalyst ((bicyclo [2.2.1]hepta-2,5-diene)[1,4-bis(diphenylphosphino)butane] rhodium(I) tetrafluoroborate, CAS 82499-43-2, STREM) in CD_3OD is prepared under argon atmosphere, and 0.6 mL of the resulting deoxygenated solution is dispatched in 5 mm NMR tubes. The 200 mM substrate concentration was chosen because biomedical applications require both a high degree of ^{13}C polarization and a high concentration to maximize the bolus of injected magnetization. On the basis of the detection sensitivity of the benchtop NMR spectrometer, we anticipate that 2 mM × % of ^{13}C spins (equating, for example, to 0.2 mM of ^{13}C-labeled substrate at $P_{^{13}C} = 10\%$ or 10 mM natural-abundance substrate at $P_{^{13}C} = 20\%$) can be readily employed for quantitative studies such as those presented here; that is, much lower substrate concentrations can be utilized.

The cold head of the p-H_2 generator is maintained at 25 K to provide a para enrichment of ~98 to 99%.[44] The p-H_2 gas is either used directly or stored for up to 4 days in aluminum tanks (~95%).[44] The experiments are performed with a simple bubbling setup using polytetrafluoroethylene (PTFE) lines pressurized with p-H_2 at 8 bar and connected with quick connect

https://doi.org/10.1021/acs.jpclett.2c00029
J. Phys. Chem. Lett. 2022, 13, 1925−1930

fittings to pressurize a 5 mm NMR tube, see Figure 1. A 1/16 in OD (1/32 in ID) catheter is used to bubble p-H_2 through the solution with a flow of 150 sccm regulated by a mass flow controller and activated by a manual valve.[45] The samples are first heated at 80 °C for 30 s (using a water bath) and then inserted into the apparatus. The hydrogenation reaction and field sweeping are performed at the center of a three-layered cylinder of the μ-metal shield, providing a magnetic field screening of 0.005 μT (5 nT).[45] There, the hydrogenation reaction is performed for 8 s with a p-H_2 flow rate of 150 sccm by closing the manual valve depicted in Figure 1. Unless stated otherwise, the magnetic field is set to a constant value of 10 μT during the reaction.

The field strength is controlled by the output signal of an arbitrary function generator (AFG1062, Tektronix, Beaverton, OR), which is directly applied to a 20 cm diameter electromagnet (XET004, XeUS Technologies, Nicosia, Cyprus[46]) sitting concentrically in the μ-metal shield (ZG-209, Magnetic Shield, Bensenville, IL), and is monitored by a three-axis fluxgate magnetometer (Mag-03, Bartington, Witney, U.K.). The field is kept constant at 10 μT during hydrogenation for 8 s, then decreases to 0 ± 5 nT to begin the constant-adiabaticity ramp of typically 4 s centered at the LAC crossing field. At the end of the constant-adiabaticity ramp, the field strength is returned to 10 μT in all cases, and the LED signals for the manual shuttling of the sample from the shields to the bore of a benchtop NMR spectrometer (1.4 T SpinSolve Carbon 60, Magritek, Wellington, New Zealand) (Figure 2).

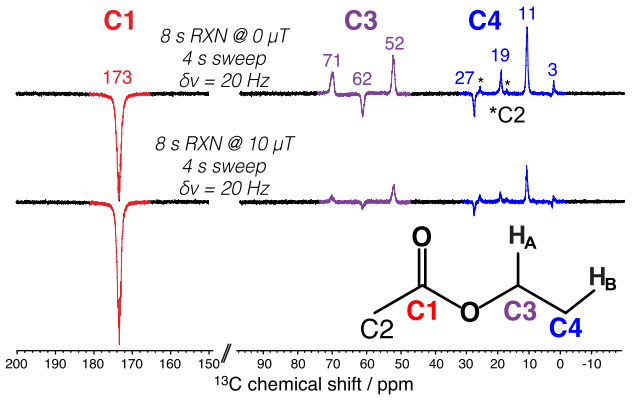

Figure 2. ^{13}C NMR spectra of HP EA recorded using a 1.4 T SpinSolve benchtop spectrometer. Top and bottom spectra correspond to different field strengths during hydrogenation (0 and 10 μT, respectively). The depicted carbon labeling is used throughout this study. The negligible carbon C2 resonances are marked with asterisks. The color-coded numbers denote ^{13}C ppm values.

The constant-adiabaticity sweep profiles are generated using the adiabatic pulse generator (APG) MATLAB program developed by Ivanov and colleagues.[42] The J coupling is set to 3.16 Hz, and a 1−100 Hz value for the difference in NMR frequencies ($\delta\nu$) is used to generate a series of waveforms of 1000 points each. The waveforms are then postprocessed so that their center matches the targeted LAC position, that is, 203 nT (Figure 3 and Figure 4a).

^{13}C NMR spectra are recorded without proton decoupling to avoid any partial collapse of potentially antiphase multiplets (Figure 2). Because of the relatively small coupling constant to protons (~6.3 Hz), C1 resonance is observed as a single line. The other carbon atoms are strongly coupled to protons via one-

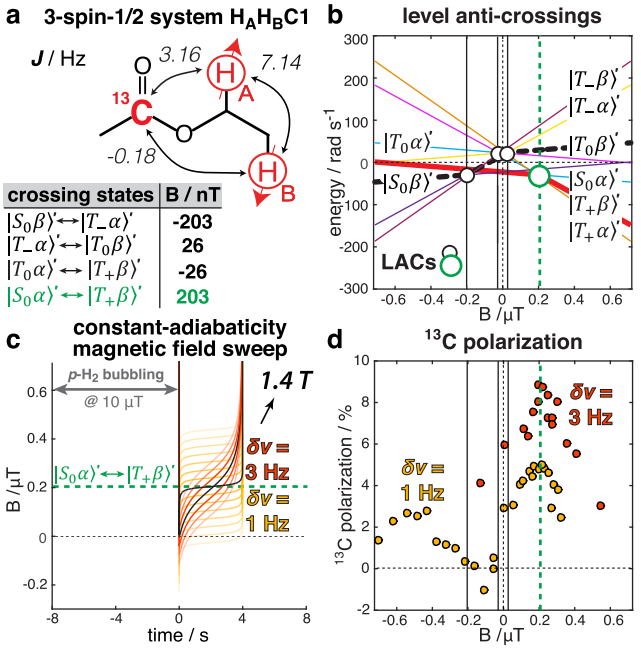

Figure 3. (a) Spin−spin couplings in the 3-spin-1/2 system H_A-H_B-C1 and B_0 field strength values of the corresponding LAC positions. (b) Eigenstates as a function of the field strength. (c) Time evolution of constant-adiabaticity magnetic field sweeps of 4 s duration and frequency differences $\delta\nu$ of 1 and 3 Hz with scan of the center field strength. (Only selected sweep traces are shown as examples.) (d) ^{13}C Polarization of carbon C1 measured as a function of the center B field at $\delta\nu$ = 1 (yellow) and 3 Hz (red).

bond spin−spin couplings, so their resonances are observed as a well-resolved methylene triplet and methyl quartets. The recorded ^{13}C HP signals are signal referenced against the ^{13}C signal of neat ethyl [1-^{13}C]acetate and converted to ^{13}C polarization ($P_{^{13}C}$), as described in detail in our recent study.[39] Pilot experiments with hydrogenation performed at 0 and 10 μT, respectively (Figure 2), show that greater $P_{^{13}C}$ for C1 is obtained in the case of a 10 μT hydrogenation field. As a result, all further experiments are performed with hydrogenation at 10 μT because our primary motivation is to maximize the ^{13}C1 polarization. Unlike ^{13}C1, other carbon sites cannot retain the HP state for minutes and have a substantially narrower ^{13}C chemical shift dispersion of downstream metabolites and therefore are poorly suited for biomedical applications.

The spin−spin couplings of the H_A-H_B-C1 3-spin-1/2 system are tabulated in Figure 3a, and the crossing states are shown in Figure 3b. The emphasis of our study is given to the C1 carbon because it has the longest *in vivo* T_1 of ~1 min. The target crossing state $|S_0\alpha\rangle' \leftrightarrow |T_+\beta\rangle'$ (*ca.* 203 nT) is indicated as the green circle in Figure 3b and is also marked by the green color in the remainder of Figure 3.

Next, we employ the magnetic sweep waveforms with $\delta\nu$ = 1 and 3 Hz to scan through the center field (Figure 3c,d). In both cases, the maximum of C1 polarization is reached at ~200 nT, although the 3 Hz ramp yields approximately twice as much as $P_{^{13}C}$ when compared with the 1 Hz ramp. This ultra-low-field scanning approach has not been previously reported to our knowledge, yet the presented data clearly show that individual LACs can be visualized (or scanned through) selectively. The selectivity is also observed with respect to the carbon of interest (^{13}C1): Figure 4b shows that the $P_{^{13}C}$ for C1 sites was several times greater than that of C3 and C4. (Note that when no ramp

https://doi.org/10.1021/acs.jpclett.2c00029
J. Phys. Chem. Lett. 2022, 13, 1925−1930

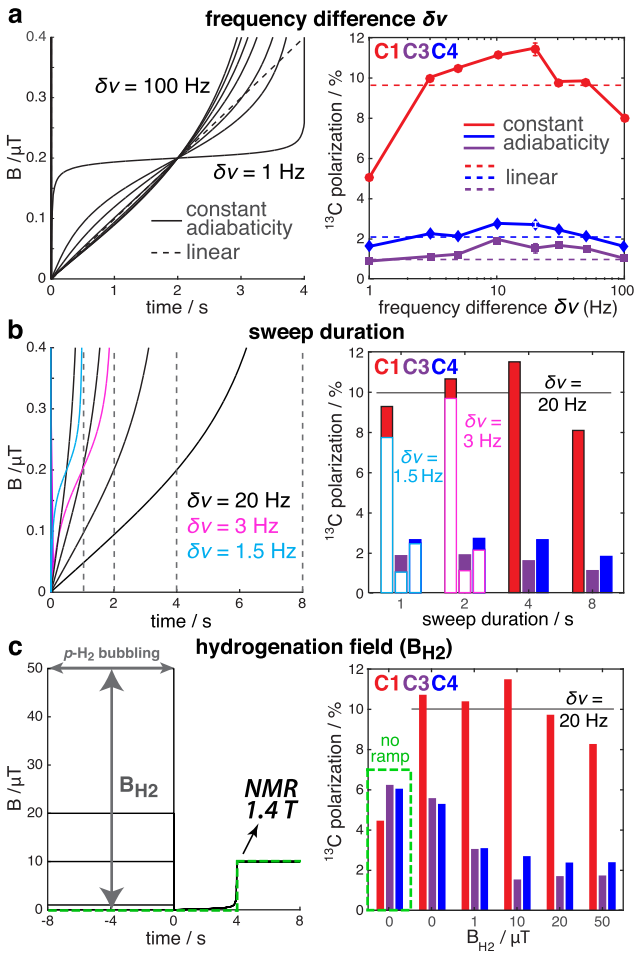

Figure 4. Constant-adiabaticity magnetic field sweeps centered at 203 nT (left) and corresponding C1, C3, and C4 polarization values detected after the sample transfer to the 1.4 T NMR detector (right) measured as a function of (a) the frequency difference $\delta\nu$ = [1−100] Hz with sweep duration = 4 s, (b) the sweep duration (from 1 to 8 s) with $\delta\nu$ = 1.5, 3, and 20 Hz, and (c) the hydrogenation magnetic field B_{H2} = [0−50] μT with $\delta\nu$ = 20 Hz. (Additional data sets are shown as white bars with cyan ($\delta\nu$ = 1.5 Hz) and magenta ($\delta\nu$ = 3 Hz) borders for 1 and 2 s durations, respectively.) In panels a and c, results obtained with a linear ramp from 0 to 400 nT in 4 s and no ramp (timed manual MFC) are shown in dashed lines, respectively. P^{13}_C values for C2 are negligible and thus are not listed.

is performed, there is virtually no selectivity; see the dashed green box in Figure 4c.) The practical utility of these observations can be potentially helpful for molecular frameworks where the information about spin−spin couplings is not readily available or in the case of more complex spin systems.

Once we have experimentally verified that the LAC of interest was selectively employed for polarization transfer from p-H_2-derived protons to the ^{13}C1 nucleus, the remainder of our studies focus on investigating the polarization transfer efficiency with respect to the experimental parameters: the frequency difference $\delta\nu$, the sweep duration, and the microtesla magnetic field during hydrogenation reaction (B_{H2}) (Figure 4). We design a series of constant-adiabaticity field ramps ranging from $\delta\nu$ = 1 to 100 Hz and compare the performance of the sequence for polarization transfer to a linear ramp also centered at ∼200 nT (Figure 4a). We find that in all cases (with the exception of too slow ($\delta\nu$ = 1 Hz) and too fast ($\delta\nu$ = 100 Hz) ramps), the constant-adiabaticity approach outperforms the linear ramp method. Whereas the gain is relatively small (a factor of ∼1.2 in the best case of $\delta\nu$ = 20 Hz), this P^{13}_C boost is appreciable and is certainly welcome in the context of potential biomedical applications of this approach. Figure 4b describes the study of the effect of the sweep duration on P^{13}_C using the optimized $\delta\nu$ = 20 Hz and $\delta\nu$ = 1.5 (cyan) and 3 Hz (magenta). There is a P^{13}_C maximum for a sweep duration of 4 s using $\delta\nu$ = 20 Hz. Note that the ramps with $\delta\nu$ = 20 Hz always result in better ^{13}C1 polarization. These findings can be rationalized as follows: Longer sweeps lead to an overall more efficient polarization transfer; however, once the sweep duration becomes appreciably long compared with the T_1 relaxation, the overall apparent P^{13}_C decreases. Finally, the parameter set ($\delta\nu$ = 20 Hz at 4 s duration) corresponding to the P^{13}_C maximum is also employed to optimize the microtesla magnetic field during the hydrogenation reaction (B_{H2}) (Figure 4c). Interestingly, it is found that 0−10 μT fields (with 10 μT being the maximum) perform better than the Earth's field of *ca.* 50 μT, which can be potentially explained by field-dependent relaxation dynamics of nuclear spins. Not using a ramp yields a markedly lower P^{13}_C for the C1 site but not for C3 and C4 (Figure 4c). The latter observation is rationalized as the loss of polarization transfer selectivity because the passage through LACs was poorly established.

Also, the HP protons readily establish radio amplification by stimulated emission of radiation (RASER) at high concentrations and high P values, making the precise P_H measurement challenging under the experimental conditions.[47−49] For a hydrogenation duration of 8 s, we estimate that P_H is ∼16−24% in the studied spin system,[50] corresponding to the estimateed polarization transfer efficiency of ∼50%, in line with the polarization transfer efficiency measured by Ivanov and coworkers.[42]

Hence, a polarization P^{13}_C of ∼12% has been demonstrated here on the targeted carbonyl C1 center of biomolecule ethyl acetate. It is anticipated that a P^{13}_C of up to 30% can be potentially achieved on many structurally similar biomolecular motifs produced via PHIP-SAH using this constant-adiabaticity approach. Specifically, the purpose-built, high-pressure hyperpolarizers (vs suboptimal p-H_2 bubbling through the 5 mm NMR tube employed here) may enable a substantially faster hydrogenation process (*e.g.*, to 4 s or less), resulting in lower P_H losses during the p-H_2 addition step and a substantially higher P_H of nascent p-H_2-derived protons than those attained in our study presented here.[51−54]

In summary, a novel experimental approach allowing for both enhanced polarization transfer efficiency between parahydrogen-derived protons and ^{13}C nuclei and LAC scanning is demonstrated with the ethyl acetate biomolecule, which is studied at natural abundance using benchtop NMR spectroscopy. This approach enables one to quickly and conveniently optimize the polarization transfer efficiency in a laboratory setting without the use of ^{13}C enrichment or high-field instrumentation and without prior knowledge of spin−spin couplings and chemical shift information. The work presented here would be of interest to those working in the broadly defined field of NMR hyperpolarization (*i.e.*, covering both hydrogenative and non-hydrogenative PHIP approaches) including physical chemists developing new sequences and hardware to enable more efficient polarization transfer from parahydrogen-derived protons to the heteronucleus (^{13}C presented here and potentially to ^{15}N and others), organic chemists developing novel synthetic approaches for preparing PHIP and SABRE precursors, present-day end users (biomedical researchers

https://doi.org/10.1021/acs.jpclett.2c00029
J. Phys. Chem. Lett. 2022, 13, 1925−1930

working on the *in vivo* application of HP contrast agents), and future end users (medical practitioners, who will one day utilize this hyperpolarization modality as a routing diagnostic tool). Overall, the presented results bode well for the future biomedical translation of constant-adiabaticity magnetic field sweeping/cycling in the context of biologically relevant molecules prepared within the PHIP-SAH framework. Finally, the presented results would also be of interest to researchers working on other expanding applications of PHIP hyperpolarization, including diagnostic applications of biofluids[55] and natural extracts.[56]

■ ASSOCIATED CONTENT

Supporting Information

The Supporting Information is available free of charge at https://pubs.acs.org/doi/10.1021/acs.jpclett.2c00029.

Transparent Peer Review report available (PDF)

■ AUTHOR INFORMATION

Corresponding Authors

Baptiste Joalland − *Department of Chemistry, Integrative Biosciences (IBio), Karmanos Cancer Institute (KCI), Wayne State University, Detroit, Michigan 48202, United States;* orcid.org/0000-0003-4116-6122; Email: joallandb@gmail.com

Eduard Y. Chekmenev − *Department of Chemistry, Integrative Biosciences (IBio), Karmanos Cancer Institute (KCI), Wayne State University, Detroit, Michigan 48202, United States; Russian Academy of Sciences, Moscow 119991, Russia;* orcid.org/0000-0002-8745-8801; Email: chekmenevlab@gmail.com

Complete contact information is available at: https://pubs.acs.org/10.1021/acs.jpclett.2c00029

Notes

The authors declare the following competing financial interest(s): E.Y.C. discloses a stake of ownership in XeUS Technologies, LTD.

■ ACKNOWLEDGMENTS

We dedicate this paper to the memory of Konstantin L. Ivanov. This work was supported by the National Science Foundation under grants CHE-1904780 and CHE-1836308, by the National Cancer Institute under 1R21CA220137, and by DOD CDMRP under BRP W81XWH-12-1-0159/BC112431.

■ REFERENCES

(1) Overhauser, A. W. Polarization of nuclei in metals. *Phys. Rev.* **1953**, *92*, 411−415.

(2) Albert, M. S.; Cates, G. D.; Driehuys, B.; Happer, W.; Saam, B.; Springer, C. S.; Wishnia, A. Biological magnetic-resonance-imaging using laser polarized Xe-129. *Nature* **1994**, *370*, 199−201.

(3) Ardenkjaer-Larsen, J. H.; Fridlund, B.; Gram, A.; Hansson, G.; Hansson, L.; Lerche, M. H.; Servin, R.; Thaning, M.; Golman, K. Increase in signal-to-noise ratio of > 10,000 times in liquid-state NMR. *Proc. Natl. Acad. Sci. U. S. A.* **2003**, *100*, 10158−10163.

(4) Golman, K.; Axelsson, O.; Johannesson, H.; Mansson, S.; Olofsson, C.; Petersson, J. S. Parahydrogen-induced polarization in imaging: Subsecond C-13 angiography. *Magn. Reson. Med.* **2001**, *46*, 1−5.

(5) Goodson, B. M. Nuclear magnetic resonance of laser-polarized noble gases in molecules, materials, and organisms. *J. Magn. Reson.* **2002**, *155*, 157−216.

(6) Kovtunov, K. V.; Zhivonitko, V. V.; Skovpin, I. V.; Barskiy, D. A.; Koptyug, I. V. Parahydrogen-induced polarization in heterogeneous catalytic processes. *Top. Curr. Chem.* **2012**, *338*, 123−180.

(7) Nikolaou, P.; Goodson, B. M.; Chekmenev, E. Y. NMR hyperpolarization techniques for biomedicine. *Chem.—Eur. J.* **2015**, *21*, 3156−3166.

(8) Kurhanewicz, J.; Vigneron, D. B.; Ardenkjaer-Larsen, J. H.; Bankson, J. A.; Brindle, K.; Cunningham, C. H.; Gallagher, F. A.; Keshari, K. R.; Kjaer, A.; Laustsen, C.; et al. Hyperpolarized ^{13}C MRI: path to clinical translation in oncology. *Neoplasia* **2019**, *21*, 1−16.

(9) Brindle, K. M. Imaging metabolism with hyperpolarized ^{13}C-labeled cell substrates. *J. Am. Chem. Soc.* **2015**, *137*, 6418−6427.

(10) Kurhanewicz, J.; Vigneron, D. B.; Brindle, K.; Chekmenev, E. Y.; Comment, A.; Cunningham, C. H.; DeBerardinis, R. J.; Green, G. G.; Leach, M. O.; Rajan, S. S.; et al. Analysis of cancer metabolism by imaging hyperpolarized nuclei: Prospects for translation to clinical research. *Neoplasia* **2011**, *13*, 81−97.

(11) Brindle, K. M.; Bohndiek, S. E.; Gallagher, F. A.; Kettunen, M. I. Tumor imaging using hyperpolarized C-13 magnetic resonance. *Magn. Reson. Med.* **2011**, *66*, 505−519.

(12) Mishkovsky, M.; Comment, A.; Gruetter, R. In vivo detection of brain krebs cycle intermediate by hyperpolarized magnetic resonance. *J. Cereb. Blood Flow Metab.* **2012**, *32*, 2108−2113.

(13) Jensen, P. R.; Peitersen, T.; Karlsson, M.; in't Zandt, R.; Gisselsson, A.; Hansson, G.; Meier, S.; Lerche, M. H. Tissue-specific short chain fatty acid metabolism and slow metabolic recovery after ischemia from hyperpolarized NMR in vivo. *J. Biol. Chem.* **2009**, *284*, 36077−36082.

(14) Mikkelsen, E. F. R.; Mariager, C. Ø.; Nørlinger, T.; Qi, H.; Schulte, R. F.; Jakobsen, S.; Frøkiær, J.; Pedersen, M.; Stødkilde-Jørgensen, H.; Laustsen, C. Hyperpolarized [1-^{13}C]-acetate renal metabolic clearance rate mapping. *Sci. Rep.* **2017**, *7*, 16002.

(15) Bastiaansen, J. A. M.; Cheng, T.; Mishkovsky, M.; Duarte, J. M. N.; Comment, A.; Gruetter, R. In vivo enzymatic activity of acetylcoa synthetase in skeletal muscle revealed by C-13 turnover from hyperpolarized 1-C-13 acetate to 1-C-13 acetylcarnitine. *Biochim. Biophys. Acta-Gen. Subj.* **2013**, *1830*, 4171−4178.

(16) Ardenkjaer-Larsen, J. H. On the present and future of dissolution-dnp. *J. Magn. Reson.* **2016**, *264*, 3−12.

(17) Bowers, C. R.; Weitekamp, D. P. Transformation of symmetrization order to nuclear-spin magnetization by chemical-reaction and nuclear-magnetic-resonance. *Phys. Rev. Lett.* **1986**, *57*, 2645−2648.

(18) Reineri, F.; Cavallari, E.; Carrera, C.; Aime, S. Hydrogenative-PHIP polarized metabolites for biological studies. *Magn. Reson. Mater. Phys.* **2021**, *34*, 25−47.

(19) Goldman, M.; Johannesson, H.; Axelsson, O.; Karlsson, M. Hyperpolarization of C-13 through order transfer from parahydrogen: A new contrast agent for MFI. *Magn. Reson. Imaging* **2005**, *23*, 153−157.

(20) Hövener, J.-B.; Pravdivtsev, A. N.; Kidd, B.; Bowers, C. R.; Glöggler, S.; Kovtunov, K. V.; Plaumann, M.; Katz-Brull, R.; Buckenmaier, K.; Jerschow, A.; et al. Parahydrogen-based hyperpolarization for biomedicine. *Angew. Chem., Int. Ed.* **2018**, *57*, 11140−11162.

(21) Kovtunov, K. V.; Koptyug, I. V.; Fekete, M.; Duckett, S. B.; Theis, T.; Joalland, B.; Chekmenev, E. Y. Parahydrogen-induced hyperpolarization of gases. *Angew. Chem., Int. Ed.* **2020**, *59*, 17788−17797.

(22) Rayner, P. J.; Duckett, S. B. Signal amplification by reversible exchange (SABRE): From discovery to diagnosis. *Angew. Chem., Int. Ed.* **2018**, *57*, 6742−6753.

(23) Kovtunov, K. V.; Pokochueva, E. V.; Salnikov, O. G.; Cousin, S.; Kurzbach, D.; Vuichoud, B.; Jannin, S.; Chekmenev, E. Y.; Goodson, B. M.; Barskiy, D. A.; et al. Hyperpolarized NMR: D-DNP, PHIP, and SABRE. *Chem. Asian J.* **2018**, *13*, 1857−1871.

(24) Bhattacharya, P.; Chekmenev, E. Y.; Perman, W. H.; Harris, K. C.; Lin, A. P.; Norton, V. A.; Tan, C. T.; Ross, B. D.; Weitekamp, D. P. Towards hyperpolarized ^{13}C-succinate imaging of brain cancer. *J. Magn. Reson.* **2007**, *186*, 150−155.

(25) Bhattacharya, P.; Chekmenev, E. Y.; Reynolds, W. F.; Wagner, S.; Zacharias, N.; Chan, H. R.; Bünger, R.; Ross, B. D. Parahydrogen-induced polarization (PHIP) hyperpolarized MR receptor imaging in vivo: A pilot study of ^{13}C imaging of atheroma in mice. *NMR Biomed.* **2011**, *24*, 1023−1028.
(26) Reineri, F.; Boi, T.; Aime, S. Parahydrogen induced polarization of ^{13}C carboxylate resonance in acetate and pyruvate. *Nat. Commun.* **2015**, *6*, 5858.
(27) Kovtunov, K. V.; Barskiy, D. A.; Salnikov, O. G.; Shchepin, R. V.; Coffey, A. M.; Kovtunova, L. M.; Bukhtiyarov, V. I.; Koptyug, I. V.; Chekmenev, E. Y. Toward production of pure ^{13}C hyperpolarized metabolites using heterogeneous parahydrogen-induced polarization of ethyl[1-^{13}C]acetate. *RSC Adv.* **2016**, *6*, 69728−69732.
(28) Kovtunov, K. V.; Barskiy, D. A.; Shchepin, R. V.; Salnikov, O. G.; Prosvirin, I. P.; Bukhtiyarov, A. V.; Kovtunova, L. M.; Bukhtiyarov, V. I.; Koptyug, I. V.; Chekmenev, E. Y. Production of pure aqueous ^{13}C-hyperpolarized acetate by heterogeneous parahydrogen-induced polarization. *Chem.—Eur. J.* **2016**, *22*, 16446−16449.
(29) Salnikov, O. G.; Chukanov, N. V.; Kovtunova, L. M.; Bukhtiyarov, V. I.; Kovtunov, K. V.; Shchepin, R. V.; Koptyug, I. V.; Chekmenev, E. Y. Heterogeneous ^{1}H and ^{13}C parahydrogen-induced polarization of acetate and pyruvate esters. *ChemPhysChem* **2021**, *22*, 1389−1396.
(30) Cavallari, E.; Carrera, C.; Aime, S.; Reineri, F. Studies to enhance the hyperpolarization level in PHIP-SAH-produced C13-pyruvate. *J. Magn. Reson.* **2018**, *289*, 12−17.
(31) Salnikov, O. G.; Chukanov, N. V.; Shchepin, R. V.; Manzanera Esteve, I. V.; Kovtunov, K. V.; Koptyug, I. V.; Chekmenev, E. Y. Parahydrogen-induced polarization of 1-^{13}C-acetates and 1-^{13}C-pyruvates using side-arm hydrogenation of vinyl, allyl and propargyl esters. *J. Phys. Chem. C* **2019**, *123*, 12827−12840.
(32) Shchepin, R. V.; Barskiy, D. A.; Coffey, A. M.; Manzanera Esteve, I. V.; Chekmenev, E. Y. Efficient synthesis of molecular precursors for para-hydrogen-induced polarization of ethyl acetate-1-^{13}C and beyond. *Angew. Chem., Int. Ed.* **2016**, *55*, 6071−6074.
(33) Cavallari, E.; Carrera, C.; Aime, S.; Reineri, F. C-13 MR hyperpolarization of lactate by using parahydrogen and metabolic transformation in vitro. *Chem.—Eur. J.* **2017**, *23*, 1200−1204.
(34) Cavallari, E.; Carrera, C.; Sorge, M.; Bonne, G.; Muchir, A.; Aime, S.; Reineri, F. The ^{13}C hyperpolarized pyruvate generated by parahydrogen detects the response of the heart to altered metabolism in real time. *Sci. Rep.* **2018**, *8*, 8366.
(35) Cavallari, E.; Carrera, C.; Aime, S.; Reineri, F. Metabolic studies of tumor cells using [1-^{13}C]pyruvate hyperpolarized by means of PHIP-side arm hydrogenation. *ChemPhysChem* **2019**, *20*, 318−325.
(36) Johannesson, H.; Axelsson, O.; Karlsson, M. Transfer of para-hydrogen spin order into polarization by diabatic field cycling. *C. R. Physique* **2004**, *5*, 315−324.
(37) Reineri, F.; Santelia, D.; Viale, A.; Cerutti, E.; Poggi, L.; Tichy, T.; Premkumar, S. S. D.; Gobetto, R.; Aime, S. Para-hydrogenated glucose derivatives as potential C-13-hyperpolarized probes for magnetic resonance imaging. *J. Am. Chem. Soc.* **2010**, *132*, 7186−7193.
(38) Chukanov, N. V.; Salnikov, O. G.; Shchepin, R. V.; Kovtunov, K. V.; Koptyug, I. V.; Chekmenev, E. Y. Synthesis of unsaturated precursors for parahydrogen-induced polarization and molecular imaging of 1-^{13}C-acetates and 1-^{13}C-pyruvates via side arm hydrogenation. *ACS Omega* **2018**, *3*, 6673−6682.
(39) Joalland, B.; Schmidt, A.; Kabir, M. S. H.; Chukanov, N. V.; Kovtunov, K. V.; Koptyug, I. V.; Hennig, J.; Hövener, J.-B.; Chekmenev, E. Y. Pulse-programmable magnetic field sweeping of parahydrogen-induced polarization by side arm hydrogenation. *Anal. Chem.* **2020**, *92*, 1340−1345.
(40) Eills, J.; Blanchard, J. W.; Wu, T.; Bengs, C.; Hollenbach, J.; Budker, D.; Levitt, M. H. Polarization transfer via field sweeping in parahydrogen-enhanced nuclear magnetic resonance. *J. Chem. Phys.* **2019**, *150*, 174202.
(41) Dagys, L.; Bengs, C.; Levitt, M. H. Low-frequency excitation of singlet−triplet transitions. Application to nuclear hyperpolarization. *J. Chem. Phys.* **2021**, *155*, 154201.
(42) Rodin, B. A.; Eills, J.; Picazo-Frutos, R.; Sheberstov, K. F.; Budker, D.; Ivanov, K. L. Constant-adiabaticity ultralow magnetic field manipulations of parahydrogen-induced polarization: Application to an AA'X spin system. *Phys. Chem. Chem. Phys.* **2021**, *23*, 7125−7134.
(43) Knecht, S.; Blanchard, J. W.; Barskiy, D.; Cavallari, E.; Dagys, L.; Van Dyke, E.; Tsukanov, M.; Bliemel, B.; Münnemann, K.; Aime, S.; et al. Rapid hyperpolarization and purification of the metabolite fumarate in aqueous solution. *Proc. Natl. Acad. Sci. U. S. A.* **2021**, *118*, e2025383118.
(44) Nantogma, S.; Joalland, B.; Wilkens, K.; Chekmenev, E. Y. Clinical-scale production of nearly pure (>98.5%) parahydrogen and quantification by benchtop NMR spectroscopy. *Anal. Chem.* **2021**, *93*, 3594−3601.
(45) Joalland, B.; Nantogma, S.; Chowdhury, M. R. H.; Nikolaou, P.; Chekmenev, E. Y. Magnetic shielding of parahydrogen hyperpolarization experiments for the masses. *Magn. Reson. Chem.* **2021**, *59*, 1180−1186.
(46) Birchall, J. R.; Nikolaou, P.; Coffey, A. M.; Kidd, B. E.; Irwin, R. K.; Murphy, M.; Molway, M.; Bales, L. B.; Goodson, B. M.; Barlow, M. J.; et al. Batch-mode clinical-scale optical hyperpolarization of xenon-129 using an aluminum jacket with rapid temperature ramping. *Anal. Chem.* **2020**, *92*, 4309−4316.
(47) Joalland, B.; Ariyasingha, N. M.; Lehmkuhl, S.; Theis, T.; Appelt, S.; Chekmenev, E. Y. Parahydrogen-induced radio amplification by stimulated emission of radiation. *Angew. Chem., Int. Ed.* **2020**, *132*, 8732−8738.
(48) Appelt, S.; Lehmkuhl, S.; Fleischer, S.; Joalland, B.; Ariyasingha, N. M.; Chekmenev, E. Y.; Theis, T. SABRE and PHIP pumped RASER and the route to chaos. *J. Magn. Reson.* **2021**, *322*, 106815.
(49) Joalland, B.; Theis, T.; Appelt, S.; Chekmenev, E. Y. Background-free proton NMR spectroscopy with radiofrequency amplification by stimulated emission radiation. *Angew. Chem., Int. Ed.* **2021**, *60*, 26298−26302.
(50) Joalland, B.; Ariyasingha, N. M.; Younes, H. R.; Nantogma, S.; Salnikov, O. G.; Chukanov, N. V.; Kovtunov, K. V.; Koptyug, I. V.; Gelovani, J. G.; Chekmenev, E. Y. Low-flammable parahydrogen-polarized MRI contrast agents. *Chem.—Eur. J.* **2021**, *27*, 2774−2781.
(51) Schmidt, A. B.; Berner, S.; Schimpf, W.; Müller, C.; Lickert, T.; Schwaderlapp, N.; Knecht, S.; Skinner, J. G.; Dost, A.; Rovedo, P.; et al. Liquid-state carbon-13 hyperpolarization generated in an MRI system for fast imaging. *Nat. Commun.* **2017**, *8*, 14535.
(52) Coffey, A. M.; Shchepin, R. V.; Feng, B.; Colon, R. D.; Wilkens, K.; Waddell, K. W.; Chekmenev, E. Y. A pulse programmable parahydrogen polarizer using a tunable electromagnet and dual channel nmr spectrometer. *J. Magn. Reson.* **2017**, *284*, 115−124.
(53) Coffey, A. M.; Shchepin, R. V.; Truong, M. L.; Wilkens, K.; Pham, W.; Chekmenev, E. Y. Open-source automated parahydrogen hyperpolarizer for molecular imaging using ^{13}C metabolic contrast agents. *Anal. Chem.* **2016**, *88*, 8279−8288.
(54) Schmidt, A. B.; Bowers, C. R.; Buckenmaier, K.; Chekmenev, E. Y.; de Maissin, H.; Eills, J.; Ellermann, F.; Glöggler, S.; Gordon, J. W.; Knecht, S.; et al. Instrumentation for hydrogenative parahydrogen-based hyperpolarization techniques. *Anal. Chem.* **2022**, *94*, 479−502.
(55) Reile, I.; Eshuis, N.; Hermkens, N.; van Weerdenburg, B. J. A.; Feiters, M. C.; Rutjes, F. P. J. T.; Tessari, M. NMR detection in biofluid extracts at sub-μM concentrations via para-H_2 induced hyperpolarization. *Analyst* **2016**, *141*, 4001−4005.
(56) Hermkens, N. K. J.; Eshuis, N.; van Weerdenburg, B. J. A.; Feiters, M. C.; Rutjes, F. P. J. T.; Wijmenga, S. S.; Tessari, M. NMR-based chemosensing via p-H_2 hyperpolarization: Application to natural extracts. *Anal. Chem.* **2016**, *88*, 3406−3412.

https://doi.org/10.1021/acs.jpclett.2c00029
J. Phys. Chem. Lett. 2022, 13, 1925−1930